JOURNAL

OF THE AMERICAN CHEMICAL SOCIETY

© Copyright 1986 by the American Chemical Society

VOLUME 108, NUMBER 16 AUGUST 6, 1986

Kinetic Studies of Carrier Transport and Recombination at the n-Silicon/Methanol Interface

Mary L. Rosenbluth and Nathan S. Lewis*

Contribution from the Department of Chemistry, Stanford University, Stanford, California 94305. *Received January 13, 1986*

Abstract: The response of the open-circuit photovoltage, V_{oc}, has been investigated with regard to changes in the minority carrier diffusion length, majority carrier density, short-circuit photocurrent density, and cell temperature of n-Si/CH_3OH junctions. The reaction kinetics are observed to be first order in dopant density, minority carrier diffusion length, and photocurrent density. The activation barrier for carrier recombination, obtained from plots of V_{oc} vs. temperature, is 1.15 ± 0.05 eV. An optimum dopant density for maximum V_{oc} is observed, and this is consistent with bulk lifetime measurements on similarly doped Si samples. The reaction kinetics are not sensitive to the concentration of redox species (at constant electrochemical potential), indicating minimal recombination losses due to poor interfacial charge transport rates. V_{oc} values for optimally doped systems (V_{oc} = 670 mV for 0.015 Ω-cm n-Si samples at 20 mA/cm^2 photocurrent densities) represent the highest photovoltages obtained to date for any n-Si-based surface barrier device. Surface recombination velocity measurements at the n-Si/CH_3OH interface have been performed, and correlations between the surface recombination rate and the improvement in current-voltage properties have been investigated.

We have recently reported that n-Si/CH_3OH photoelectrochemical cells exhibit open-circuit voltages, V_{oc}, in excess of 630 mV under Air Mass 1 irradiation conditions.[1] These photovoltages compare favorably with the best values obtained in advanced solid-state silicon cell designs,[2-6] and far exceed the V_{oc} values reported for other n-Si-based surface barrier devices.[7-11] The superior behavior of these liquid junctions has been ascribed in part to the oxide overlayer formed at the Si surface in CH_3OH solvent.[1,12-14] We report here kinetic transport studies of carrier recombination at these junctions.

These studies address several important questions in the field of semiconductor/liquid junction chemistry. It is generally hypothesized that semiconductor/liquid interfaces will not yield solar photovoltaic efficiencies which are as high as those obtained with the best diffused junction solid-state devices. Potential advantages of the semiconductor/liquid system are generally thought to lie with the use of polycrystalline or thin film substrates[15-17] or perhaps in applications such as integrated solar photovoltaic/electrochemical production of fuels.[18,19] In contrast, our studies on the n-Si/CH_3OH interface demonstrate that certain semiconductor/liquid interfaces can produce junctions with V_{oc} values in accord with ideal diode theory. These V_{oc} values exceed photovoltages demonstrated for typical diffused n-p$^+$ Si junction systems because of decreased junction and front-surface recombination losses. The transport studies reported here elucidate the mechanistic features of carrier recombination at these semiconductor/liquid interfaces and address the limitations, if any, on V_{oc} values attainable in the n-Si/CH_3OH system due to surface-related recombination processes.

We also describe measurements of the surface recombination velocity of n-Si/CH_3OH interfaces. The ratio of surface recom-

* Author to whom correspondence should be addressed.

(1) Rosenbluth, M. L.; Lieber, C. M.; Lewis, N. S. *Appl. Phys. Lett.* **1984**, *45*, 423.
(2) (a) Blakers, A. W.; Green, M. A.; Jiqun, S.; Keller, E. M.; Wenham, S. R.; Godfrey, R. B.; Szpitalak, T.; Willison, M. R. *IEEE Electron Device Lett.* **1984**, *EDL-5*, 12. (b) Godfrey, R. B.; Green, M. A. *Appl. Phys. Lett.* **1979**, *34*, 791. (c) Blakers, A. W.; Green, M. A. *Appl. Phys. Lett.* **1981**, *39*, 483.
(3) Fahrenbruch, A. L.; Bube, R. H. *Fundamentals of Solar Cells*; Academic: New York, 1983.
(4) Bae, M. S.; D'Aiello, R. V. *Appl. Phys. Lett.* **1977**, *31*, 285.
(5) Garner, C. M.; Sexton, F. W.; Nasby, R. D. *Sol. Cells* **1981**, *4*, 37.
(6) Fang, C. R.; Hauser, J. R. *Proc.—IEEE Photovolt. Spec. Conf.* **1978**, *13*, 1318.
(7) (a) Legg, K. L.; Ellis, A. B.; Bolts, J. M.; Wrighton, M. S. *Proc. Natl. Acad. Sci. U.S.A.* **1977**, *74*, 4116. (b) Chazalviel, J. N.; Truong, T. B. *J. Electroanal. Chem.* **1980**, *114*, 299. (c) Malpas, R. E.; Itaya, K.; Bard, A. J. *J. Am. Chem. Soc.* **1981**, *103*, 1622. (d) Fan, F.-R. F.; Keil, R. G.; Bard, A. J. *J. Am. Chem. Soc.* **1983**, *105*, 220. (e) Fan, F.-R. F.; Shea, T. V.; Bard, A. J. *J. Electrochem. Soc.* **1984**, *131*, 828.
(8) (a) Ponpon, J. P.; Siffert, P. *J. Appl. Phys.* **1976**, *47*, 3248. (b) Howe, A. J. *J. Chem. Soc., Chem. Commun.* **1983**, 1407.
(9) Ghosh, A. K.; Fishman, C.; Feng, T. *J. Appl. Phys.* **1978**, *49*, 3490.
(10) Fonash, S. J. *Solar Cell Device Physics*; Academic: New York, 1981.
(11) Sze, S. M. *Physics of Semiconductor Devices*, 2nd ed.; Wiley: New York, 1981.
(12) Gronet, C. M.; Lewis, N. S.; Cogan, G.; Gibbons, J. *Proc. Natl. Acad. Sci. U.S.A.* **1983**, *80*, 1152.
(13) Cogan, G. W.; Gronet, C. M.; Gibbons, J. F.; Lewis, N. S. *Appl. Phys. Lett.* **1984**, *44*, 539.
(14) Lewis, N. S. *J. Electrochem. Soc.* **1984**, *131*, 2496.
(15) (a) Wrighton, M. S. *Chem. Eng. News* **1979** (*Sept 3*), *1*, 29. (b) Parkinson, B. *J. Chem. Educ.* **1983**, *60*, 338.
(16) Hodes, G.; Fonash, S. J.; Heller, A.; Miller, B. *Adv. Electrochem. Electrochem. Eng.* **1984**, *13*, 113.

0002-7863/86/1508-4689$01.50/0 © 1986 American Chemical Society

bination to net interfacial charge transfer is an important factor in determining the efficiency of a semiconductor/liquid junction.[10,20] Nelson et al. have shown that chemical treatments which increase the efficiency of n-GaAs/Se^{2-}–KOH junctions are also effective at reducing the surface recombination velocity at the n-GaAs/air interface.[21] In contrast, Gottesfeld and Feldberg have found no correlation between improvements in efficiency resulting from chemical treatments of CdSe/liquid interfaces and the high-level injection surface recombination velocities of these systems.[22] Such measurements are of interest for the n-Si/CH_3OH system in order to ascertain whether the excellent current–voltage properties correlate with a low surface recombination velocity.

Our studies of the Si/liquid junction are also valuable in elucidating the interfacial chemistry which occurs in Si Schottky barrier formation. Typical n-Si/metal junctions display poor photovoltages (V_{oc} = 0.3 V at photocurrent densities of 20 mA/cm^2) from pinning of the Fermi level as a result of metal silicide formation.[11] The improvements in V_{oc} seen with photoelectrochemical treatment of the n-Si/CH_3OH system qualitatively resemble increases in V_{oc} observed in some metal/oxide (insulator)/semiconductor (MIS) solar cell structures.[10,23] However, the improvements attained to date for n-Si MIS systems have not reached the V_{oc} values of the n-Si/CH_3OH liquid junction system, and the mechanism of V_{oc} improvement in MIS cells is still controversial.[10,24,25] A direct comparison of the transport behavior of n-Si/liquid junctions and n-Si/insulator/metal MIS systems is one of the goals of our study.

Experimental Section

A. Sample Characterization and Electrode Preparation. The Czochralski-grown samples used in these experiments were optically polished, n-type, (100)-oriented, single-crystal wafers made by Siltec and Monsanto. The float-zone, (100)-oriented, 0.2 and 100–150 Ω-cm crystals were supplied by Prof. Richard Swanson of Stanford University. A Tencor Instruments four-point probe was used to determine wafer resistivities, and dopant densities were then calculated utilizing the data of Thurber et al.[26]

Electrodes were fashioned from 4 × 4 mm Si squares, as described previously.[1,12] For the surface recombination velocity determinations, both a Schottky barrier and an ohmic contact were needed on the unpolished side of the Si samples. The Schottky barriers were made by evaporation of 99.999% Au dots in a vacuum of base pressure $\leq 5 \times 10^{-6}$ torr. These Schottky barriers were encircled by a Ga–In eutectic ring.

B. Photoelectrochemical Cell Techniques. The photoelectrochemical experiments were performed in a single-compartment air-tight Pyrex cell, and illumination was obtained from an ELH-type tungsten–halogen bulb (3250 K color temperature, dichroic rear reflector).[27] Immediately before use, all electrodes were etched with 49% HF (semiconductor grade) and dried in a stream of nitrogen. Current–voltage characteristics were obtained as described previously.[1,12]

V_{oc}–J_{sc} measurements were performed by two procedures. In one method, I–V data were collected at various light intensities, and V_{oc} and J_{sc} values were obtained directly from the current–voltage properties with the aid of a Keithley four-digit voltmeter. For extremely low forward bias (<0.3 V), a parallel resistance component in the I–V behavior was observed, and this data (with a higher diode quality factor) was not included in the V_{oc}–J_{sc} analysis described in this work. For the highest light intensities used in this study (≫100 mW/cm^2), substantial concentration polarization and series resistance overpotentials were observed. This problem was minimized by assuming that J_{sc} was proportional to the incident light intensity; thus, plots of V_{oc} (measured with a voltmeter) vs. incident intensity were directly correlated with V_{oc}–J_{sc} plots. The irradiation was provided at 514.5 nm by an Ar ion laser, and the expanded beam was uniform in intensity (±10%) over the entire photoelectrode area. At modest photocurrent densities, where accurate data could be obtained by both procedures, agreement between the two methods was excellent.

V_{oc} vs. T measurements were performed in an air-tight Pyrex cell which was immersed in a silvered Dewar with a transparent slit. The Dewar was filled with ethanol, and the desired level of illumination was obtained through the Dewar slit with an ELH bulb. In order to control the cell temperature, copper tubing was wound around the cell inside the Dewar, and a controlled flow of liquid nitrogen was pumped through the Cu coil. Temperatures were measured with an Omega Co. copper–constantan Type T thermocouple which was immersed in the electrochemical cell. V_{oc} was determined with a high-impedance voltmeter as the voltage between the illuminated semiconductor electrode and a Pt reference electrode.

Determination of the surface recombination velocity required lock-in analysis (PAR Model 124A) of the photovoltage and photocurrent signals. The reference potential for the surface recombination velocity determinations was a single junction standard calomel electrode. Similar circuitry was utilized for the spectral response measurements.

Some surface recombination velocity measurements were determined under high-level injection conditions. The excitation source was a stroboscope, and the surface conductivity was monitored using a contactless microwave photoconductivity technique.[28] Unfortunately, the decay transients were out of the instrumentation range for both HF-etched and photoelectrochemically treated samples (S_f > 100-cm/s).

C. Optical Techniques. The optical hardware for the diffusion length, spectral response, and surface recombination velocity experiments consisted of a Spex, Inc., 1682A radiation source and a Spex 1681B monochromator (with 0.5-mm slits). The light was chopped by a 13-Hz Type STA-5AR chopper from American Time Products. A calibrated Si photodiode (United Detector Technology) was used as a standard for the signal channel. Another Si photodiode measured a beam-split portion of the illumination, and this diode served as a continuous calibration of the lamp intensity. Signals were obtained with independent lock-in detection of the sample and calibration channels.

D. Chemicals and Electrolytes. All of the redox couples used [$MV^{2+/+}$ (MV = *N,N'*-dimethyl-4,4'-bipyridinium, $BV^{2+/+}$ (BV = *N,N'*-dibenzyl-4,4'-bipyridinium), $Fc^{+/0}$ (Fc = ferrocene), $AcFc^{+/0}$ (AcFc = acetylferrocene), $TMPD^{+/0}$ (TMPD = *N,N,N',N'*-tetramethylphenylenediamine), $Me_2Fc^{+/0}$ (1,1'-dimethylferrocene), $CoCp_2^{+/0}$ (cobaltocene), and $Me_{10}Fc^{+/0}$ (bis(pentamethylcyclopentadienyl)iron)] were purified by recrystallization or sublimation. The substituted cobalticinium compounds were synthesized according to the procedures of Sheats and Rausch.[29] The resulting PF_6^- salts were converted to Cl^- salts (for solubility in alcohols) by ion-exchange chromatography with DEAE-Sephadex A-50 resin.

All solids were loaded into the cells in the nitrogen atmosphere of a Vacuum Atmospheres, Inc., drybox. After addition of the solids, methanol (distilled from Mg and stored over 3-Å molecular sieves) was introduced into the cell via syringe techniques. All subsequent manipulations with the electrochemical cell were performed under a nitrogen atmosphere, except where otherwise noted.

Results and Discussion

A. Spectral Response Properties and Determination of Minority Carrier Diffusion Length. A crucial materials parameter for characterization of a semiconductor/liquid junction is the semiconductor minority carrier diffusion length, L_p (for an n-type sample). For Si, the appropriate value for L_p can be determined from surface photovoltage measurements[30,31] and/or from the spectral response of the n-Si/CH_3OH–Me_2Fc–Me_2Fc^+ cell in the region between 800 and 1100 nm. For Si wafers with ρ > 0.2 Ω-cm, the thickness, d, of the Si wafer is also an important variable, because the minority carrier diffusion length can often exceed the wafer thickness, yielding an "effective" L_p value of approximately $d/2$.[30]

(17) Heller, A.; Miller, B.; Chu, S. S.; Lee, Y. T. *J. Am. Chem. Soc.* **1979**, *101*, 7633.
(18) (a) Rajeshwar, K. *J. Appl. Electrochem.* **1985**, *15*, 1. (b) Rajeshwar, K.; Singh, P.; DuBow, J. *Electrochim. Acta* **1978**, *23*, 1117.
(19) Parkinson, B. *Acc. Chem. Res.* **1984**, *17*, 431 and references therein.
(20) (a) Peter, L. M. *Electrochemistry* **1984**, *9*, 66. (b) Reichman, J. *Appl. Phys. Lett.* **1980**, *36*, 574. (c) Haneman, D.; McCann, J. F. *J. Electrochem. Soc.* **1982**, *129*, 1134. (d) Albery, W. J.; Bartlett, P. N.; Hamnett, A.; Dare-Edwards, M. P. *J. Electrochem. Soc.* **1981**, *128*, 1492. (e) Wilson, R. H. *J. Appl. Phys.* **1977**, *48*, 4292.
(21) Nelson, R. J.; Williams, J. S.; Leamy, H. J.; Miller, B.; Parkinson, B.; Heller, A. *Appl. Phys. Lett.* **1980**, *36*, 76.
(22) Evanor, M.; Gottesfeld, S.; Harzion, Z.; Huppert, D.; Feldberg, S. F. *J. Phys. Chem.* **1984**, *88*, 6213.
(23) (a) Green, M. A.; Godfrey, R. B. *Appl. Phys. Lett.* **1976**, *29*, 610. (b) Hanselaer, P. L.; Laflere, W. H.; Van Meirhaeghe, R. L.; Cardon, F. *J. Appl. Phys.* **1984**, *56*, 2309.
(24) Pulfrey, D. L. *IEEE Trans. Electron Device* **1978**, *ED-25*, 1308.
(25) Singh, R.; Green, M. A.; Rajkanan, K. *Sol. Cells* **1981**, *3*, 95.
(26) Thurber, W. R.; Mattis, R. L.; Liu, Y. M.; Filliben, J. J. *J. Electrochem. Soc.* **1980**, *127*, 1807.
(27) Matson, R. J.; Emery, K. A.; Bird, R. E. *Sol. Cells* **1984**, *11*, 105.
(28) *Annu. Book ASTM Stand.* **1981**, *F28-75*, 195.
(29) Sheats, J. E.; Rausch, M. D. *J. Org. Chem.* **1970**, *35*, 3245.
(30) *Annu. Book ASTM Stand.* **1978**, *F-391-78*, 795.
(31) Garrett, C. B.; Brattain, W. H. *Phys. Rev.* **1955**, *99*, 376.

Table I. Transport Data for the n-Si/$Me_2Fc^{+/0}$–$LiClO_4$–CH_3OH Interfaces

resistivity, Ω-cm	L_p,[a] μm	V_{oc} (theory),[b] mV	V_{oc} (exptl),[c] mV	V_{oc} (0.0 K),[d] V	$-\partial V/\partial T$ (theory),[e] mV/K	$-\partial V/\partial T$ (exptl),[f] mV/K
1.5	190	568	565	1.20	2.11	2.20 ± 0.10
0.6	165	592	593	1.20	2.03	2.0 ± 0.05
0.2	195	635	635	1.22	1.89	1.94 ± 0.05
0.015	17	670	670	1.21	1.76	1.80 ± 0.05
0.0025	1[g]	579	230	h	2.07	h

[a] Determined from near-infrared spectral response properties (Figures 1 and 2). [b] Calculated from eq 2; J_{sc} = 20.0 mA/cm², T = 300 K in all cases. [c] Error is ±5 mV for various samples at J_{sc} = 20.0 mA/cm². [d] Extrapolated from V_{oc} vs. T data for 200–300 K. Typically over 300 data points were collected; correlation coefficients were always >0.999. Range in intercept is ±50 mV for a number of determinations. Intercept overestimates the activation barrier by 5% due to contributions from the log term in eq 2.[3] [e] Calculated from V_{oc} (theory) at 300 K and an intercept at 0 K of 1.20 V[3]. [f] Slopes of V_{oc} vs. T plots in the range 200–300 K. Errors reflect variation from sample to sample. [g] Calculated from literature data.[34,35] [h] Nonlinear V_{oc} vs. T behavior.

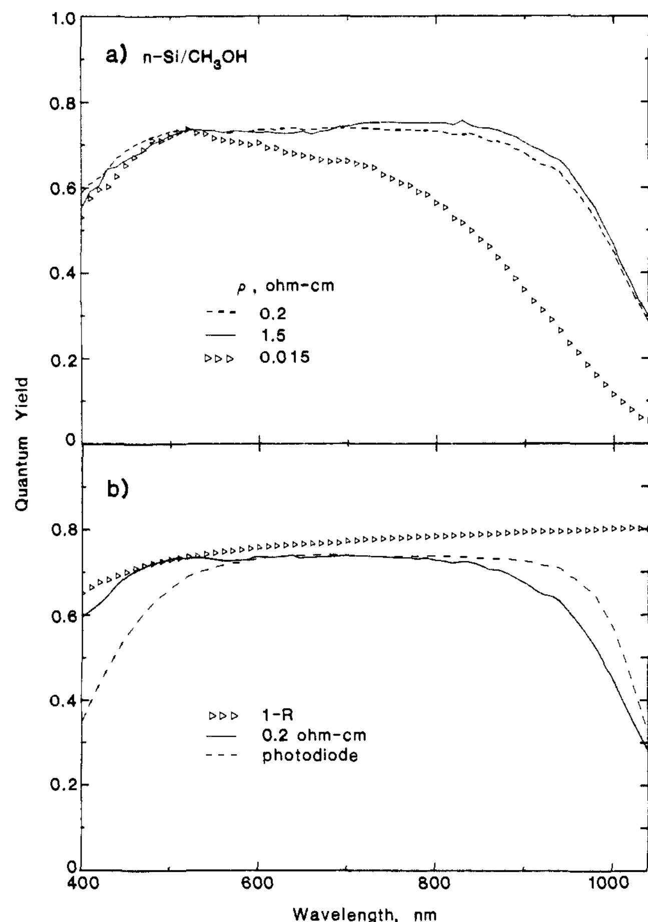

Figure 1. (a) Short-circuit quantum yield as a function of wavelength for n-Si samples of different resistivities in 5.0 mM Me_2Fe–0.5 mM Me_2Fc^+–1 M $LiClO_4$–CH_3OH: (---) 0.2 Ω-cm; (—) 1.5 Ω-cm; (Δ) 0.015 Ω-cm. (b) Comparison of the short-circuit spectral response properties of (—) 0.2 Ω-cm n-Si/$Me_2Fc^{+/0}$–$LiClO_4$–CH_3OH and (---) p–n⁺ United Detector Technology photodiode. The curve of (1 – reflectivity) of the n-Si/CH_3OH junction (Δ) is included as an indication of the theoretical limit on the external quantum yield.

Under the conditions that $L_p \gg W$ (W = depletion width) and that there is negligible recombination in the depletion region at short circuit (both reasonable assumptions for single-crystal Si), the spectral response, η, for $\alpha(\lambda)^{-1} \gg$ W (α = optical absorption coefficient, cm⁻¹) can be approximated by eq 1.[32]

$$\eta_{int} = \frac{1}{1 + \dfrac{1}{\alpha(\lambda)L_p}} \quad (1)$$

Thus, a plot of the reciprocal of the internal quantum yield, η_{int} (i.e., the quantum yield after correction for the reflectivity and transmission losses of all optical interfaces), vs. $1/\alpha(\lambda)$ should

(32) Gartner, W. W. *Phys. Rev.* **1959**, *116*, 84.

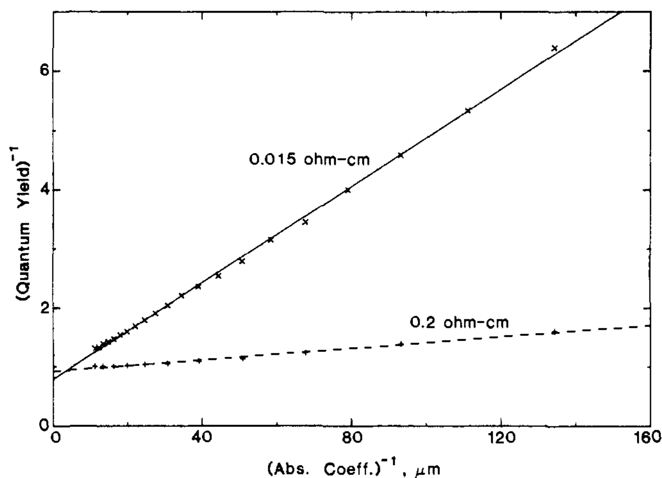

Figure 2. Near-IR spectral response data ($1/\eta_{int}$ vs. $1/\alpha(\lambda)$) for wavelengths 800 nm ≤ λ ≤ 1000 nm taken from the curves of Figure 1a: (---) 0.2 Ω-cm; (—) 0.015 Ω-cm. The slope and x intercept of each line give the value of the minority carrier diffusion length of the sample according to eq 1. L_p for the 0.2 Ω-cm sample = 195 μm; L_p for the 0.015 Ω-cm sample = 17 μm.

yield a straight line, and both the slope and the negative intercept on the abcissa should yield values for an effective L_p. Accurate values for $\alpha(\lambda)$ and for the reflectivity of stress-relieved Si were obtained from literature data.[30,33]

Figure 1a displays the external quantum yield of the n-Si/CH_3OH system vs. wavelength for several mirror-finished, (100)-oriented n-Si samples. For these experiments, we have employed very low concentrations of Me_2Fc/Me_2Fc^+ and short optical path lengths, in order to minimize optical absorption losses in the liquid. Plots of $1/\eta_{int}$ vs. $1/\alpha(\lambda)$ obtained from these data are depicted in Figure 2. For samples with $\rho \geq 0.2$ Ω-cm, we find L_p values on the order of $^1/_2$ the wafer thickness, indicating high carrier lifetimes in these unprocessed wafers.

We observe much smaller L_p values for the 0.015 and 0.0025 Ω-cm samples (Figures 1 and 2; Table I). Auger recombination processes can establish an upper limit to the minority carrier lifetime for highly doped semiconductors,[3] and such processes are well-known for Si samples at these high doping levels. Our L_p values for these samples are in good agreement with expectations based on the literature values for the Auger coefficients and minority carrier mobilities.[34] This decreased lifetime with increases in N_D (majority carrier density) will impose an upper limit on the V_{oc} which can be attained for n-Si systems at 300 K and is reflected in the photovoltage data discussed in section B.

The response of the samples in the blue region gives an indication of the limitations due to surface recombination. Spectral response data for our samples exhibit little loss in efficiency as compared to a typical p–n⁺ photodiode (Figure 1b). Much of the

(33) (a) Runyan, W. R. Southern Methodist Universtiy Report/NASA Report CR 93154, 1967, 83-13; Southern Methodist University, Dallas. (b) Aspnes, D. E.; Studna, A. A. *Phys. Rev. B: Condens. Matter* **1983**, *B27*, 985.

(34) (a) Dziewior, J.; Schmid, W. *Appl. Phys. Lett.* **1977**, *31*, 346. (b) Dziewior, J.; Silber, D. *Appl. Phys. Lett.* **1979**, *35*, 170.

decline in η_{ext} for $\lambda < 430$ nm can be explained by an increase in reflectivity at short wavelengths. Studies are under way to correlate the n-Si/CH_3OH spectral response properties with the ratio of net interfacial charge transfer to surface recombination losses as modeled by Green.[35]

B. Dependence of V_{oc} on Dopant Density. Important variables in interfacial kinetic studies include N_D, L_p, the photocurrent density (J_{ph}), and the cell temperature (T). For n-Si samples with $\rho = 1.5$ Ω-cm ($N_D = 3.3 \times 10^{15}$ cm^{-3}), we have previously observed that the extrapolated intercept of a V_{oc} vs. T plot for the n-Si/$Me_2Fc^{+/0}$-$LiClO_4$-CH_3OH cell was 1.1–1.2 V.[1] We also observed[1] that decreases in sample resistivity, up to our previous limit of $\rho = 0.2$ Ω-cm, led to improved V_{oc} values. We report further kinetic characterization of this system below.

Table I summarizes the dependence of V_{oc} on N_D and T for a number of (100)-oriented n-Si samples. For these experiments, the light intensity has been adjusted to achieve a short-circuit photocurrent density of 20.0 mA/cm^2 at room temperature. For $\rho \geq 0.015$ Ω-cm, excellent agreement is obtained between experimental data and the theoretical expectations for limitations on V_{oc} by a bulk diffusion/recombination process, eq 2.[1,3,36,37]

$$V_{oc} = \frac{kT}{q} \ln \frac{J_{ph}N_DL_p}{qD_pN_CN_V} + \frac{E_g}{q} \quad (2)$$

D_p is the hole diffusion coefficient, E_g is the band-gap energy, and N_C and N_V are the effective density of states in the conduction and valence band, respectively. For the series of samples used in this study, the V_{oc} is largest at $\rho \sim 0.015$ Ω-cm and declines to very low ($V_{oc} < 0.3$ V) values for the $\rho = 0.0025$ Ω-cm sample at room temperature. This indicates that there is an optimum dopant density for efficient photovoltaic response at the n-Si/CH_3OH interface.

This V_{oc} vs. N_D behavior can be contrasted with typical Schottky barrier systems, where V_{oc} depends on the barrier height and consequently has little dependence on N_D.[3,10,11] The 670 ± 5 mV V_{oc} value obtained with 0.015 Ω-cm substrates is the highest reported photovoltage at $J_{sc} = 20.0$ mA/cm^2 and 300 K for any n-type Si-based solar device to date. The limitations on the photovoltage in this sample result from band-gap narrowing at these high doping levels[38] combined with the modest diffusion length of the sample under study. Further optimization of the materials parameters as dictated by eq 2 is predicted to result in increased V_{oc} values. For solar applications, the 0.015 Ω-cm samples display relatively poor quantum yields in the near-infrared region; thus, less highly doped samples (probably between 0.15 and 0.05 Ω-cm) with back surface fields would provide a superior combination of V_{oc} and J_{sc} under solar illumination.

The decline in V_{oc} for the 0.0025 Ω-cm sample cannot be explained by diffusion length limitations on a bulk recombination/diffusion mechanism. This decline indicates the onset of surface-oriented recombination processes for this highly degenerate semiconductor sample ($N_D = 2.7 \times 10^{19}$ cm^{-3}; $E_f = E_C + 13$ mV). The interfacial properties of these degenerate systems are expected to represent another regime of recombination rate control and can lead to substantially lower V_{oc} values and higher leakage currents than are observed for higher resistivity samples. We observe substantially poorer rectification properties and increased dark currents from these degenerately doped samples. This behavior is similar to that reported in studies of several other semiconductor/liquid junctions, where the semiconductor has been doped to near degeneracy.[39] Our data clearly indicate that the interface parameters observed for such highly doped samples should not necessarily be taken to represent the behavior obtained from all types of semiconductor/liquid samples, even if the semiconductor is exposed to identical surface pretreatment procedures.

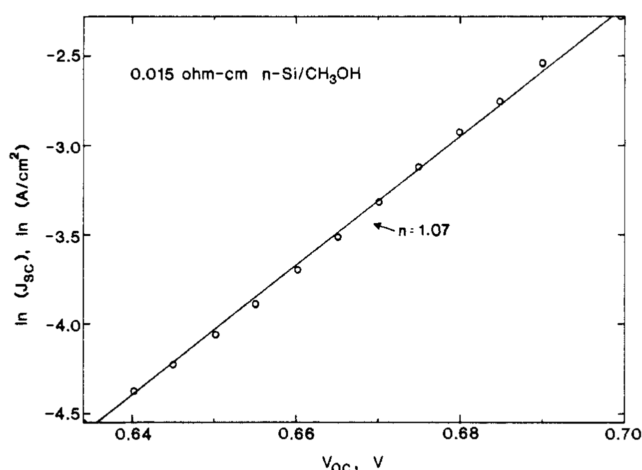

Figure 3. Natural logarithm of the short-circuit photocurrent density vs. the open-circuit photovoltage for 0.015 Ω-cm n-Si in 0.2 M Me_2Fc–10.0 mM Me_2Fc^+–1.0 M $LiClO_4$–CH_3OH liquid junction cells. The slope of the line yields a diode quality factor of 1.07; typically we observe quality factors of 1.05 ± 0.1. Limitations on V_{oc} by a bulk recombination/diffusion mechanism predict a diode quality factor of 1.0.

C. J–V Behavior and Mechanistic Data for Carrier Transport Processes. The assertion of control of kinetics in the n-Si/$Me_2Fc^{+/0}$–CH_3OH system by bulk recombination/diffusion limitations via eq 2 implies that the diode quality factor should be 1.0. Such near-ideal quality factors (i.e., Tafel slopes of 59 mV/decade of current) are rarely observed for semiconductor/liquid interfaces. We have determined the quality factor by plotting the logarithm of the incident light intensity vs. the photovoltage. This method minimizes effects of series resistance and concentration overpotential losses which plague dark ln (J) – V measurements. Additionally, the interface transport kinetics might be different when injection is obtained by an applied bias as opposed to injection from illumination, and the latter situation is more relevant to the photocurrent–voltage behavior of interest in this study.

Plots of the natural log of the light intensity vs. photovoltage are displayed in Figure 3 for a 0.015 Ω-cm sample. We observe quality factors of 1.05 ± 0.1 over the measured voltage range. Similar data have been obtained for 1.5 cm and 0.2 Ω-cm (100)-oriented n-Si samples. Verification of the intensity–voltage data at the lower light intensities has been obtained by direct I–V measurements of J_{sc} and V_{oc} for each light intensity. We note that there appears to be no deviation from linearity in these plots even up to V_{oc} values approaching 700 mV for the 0.015 Ω-cm sample. This indicates that there are no intrinsic limitations in the n-Si/CH_3OH system which would prevent attainment of open-circuit voltages greater than 700 mV under AM1 conditions, if samples with the proper combination of dopant density and lifetime could be obtained. These plots also indicate that potential drops across the Helmholtz layer and/or any Si overlayers do not deleteriously affect the transport processes at the n-Si/CH_3OH interface.

D. Temperature Dependence of V_{oc}. Table I also contains data concerning the temperature dependence of V_{oc} at fixed illumination intensity. When eq 2 applies, an intercept of 1.1–1.2 V at 0 K is predicted, and the slope is predicted to vary with changes in L_p and N_D. Data presented previously for 1.5 Ω-cm n-Si samples were consistent with eq 2 as the dominant recombination mechanism;[1] however, it is also possible that the temperature dependence originates from the variation of solution redox potential with temperature,[40] from a change in E_g with T,[11] or from some other

(35) (a) Green, M. A. *J. Appl. Phys.* **1976**, *47*, 547. (b) Green, M. A. *J. Appl. Phys.* **1979**, *50*, 1116.
(36) Shockley, W. *Bell. Syst. Tech. J.* **1949**, *28*, 435.
(37) Lewis, N. S. *Annu. Rev. Mater. Sci.* **1984**, *14*, 95.
(38) Lanyon, H. P. D.; Tuft, R. A. *IEEE Trans. Electron Device* **1979**, *ED-26*, 1014.
(39) (a) Kohl, P. A.; Bard, A. J. *J. Electrochem. Soc.* **1979**, *126*, 598. (b) Kohl, P. A.; Bard, A. J. *J. Electrochem. Soc.* **1979**, *126*, 59. (c) Bolts, J. M.; Wrighton, M. S. *J. Am. Chem. Soc.* **1979**, *101*, 6179. (d) Baglio, J. A.; Calabrese, G. S.; Harrison, D. J.; Kamieniecki, E.; Ricco, A. J.; Wrighton, M. S.; Zoski, G. D. *J. Am. Chem. Soc.* **1983**, *105*, 2246.
(40) (a) Yee, E. L.; Cave, R. J.; Guyer, K. L.; Tyma, P. D.; Weaver, M. J. *J. Am. Chem. Soc.* **1979**, *101*, 1131. (b) Hupp, J. T.; Weaver, M. J. *Inorg. Chem.* **1984**, *23*, 3639.

Table II. Effect of Concentration on V_{oc}

entry	$[Me_2Fc]$, M	$[Me_2Fc]^+$, M	V_{oc}, mV[a]
1	0.20	0.0010	641
2	0.20	0.0050	642
3	0.20	0.0100	643
4	0.10	0.0050	643
5	0.010	0.0005	645[b]

[a] 0.2 ohm-cm (100) n-Si in 1.0 M $LiClO_4$–CH_3OH at 18 °C. J_{sc} = 20 mA/cm². [b] Measured at 70 mW/cm² incident light intensity; J_{sc} data unavailable due to mass transport limitations. For comparison, 70 mW/cm² in entry 1 yielded J_{sc} = 18.3 mA/cm², and there is slightly less optical loss in the solution of entry 5.

temperature-dependent parameter. The new data in Table I implies minimal effects from changes in the barrier height in response to temperature, because we observe the predicted variation in slope in response to changes in the bulk properties of the semiconductor. Consistently, the maximum V_{oc} measured at 210 K (at illumination intensities of approximately 10 suns) is > 800 mV, indicating transport activation barriers substantially in excess of this value.

Additionally, we have directly measured the temperature dependence of $E^{\circ\prime}$ for Me_2Fc/Me_2Fc^+ in CH_3OH solvent by the nonisothermal cell method.[40] We find a small temperature dependence of $E^{\circ\prime}(Me_2Fc^{+/0})$ (–0.1 mV/(deg K)) such that increases in temperature produce more negative electrochemical potentials, i.e., slightly lower barrier heights. However, throughout this temperature range, the electrochemical potential remains in the region where the 300 K V_{oc} for oxidized n-Si has negligible dependence on $E(A^+/A)$ (vide infra). These results thus indicate that changes in barrier height with temperature are not the cause of the dependence of V_{oc} on cell temperature.

We also rule out substantial effects from changes in photocurrent density with temperature under our conditions of constant incident light intensity. The temperature dependence of the absorption coefficient, the reflectivity, the minority carrier lifetime, the majority carrier mobility, and the band gap have been determined for silicon;[11,41] therefore, the temperature dependence of the ideal photocurrent can be calculated. Furthermore, the temperature dependence of the photocurrent in actual diffused Si p–n junction systems has been measured.[41,42] The variations in short-circuit current density under tungsten–halogen irradiation are small (ΔJ_{ph} < 2 mA/cm² from 200 to 300 K) and produce logarithmic changes in V_{oc}. For comparison to the data in Table I, a conventional diffused p–n$^+$ junction with a base resistivity of 1 Ω-cm ($N_A = 1.5 \times 10^{16}$ cm^{-3}) with a V_{oc} = 610 mV at 294 K shows a temperature coefficient $\partial V_{oc}/\partial T$ = –2.05 mV/(deg K) at room temperature.[41]

E. Effects of Solution Redox Species Concentrations on Interfacial Transport Rates for the n-Si/$Me_2Fc^{+/0}$–CH_3OH System. We have investigated the possible effects of poor electron-transfer kinetics at the semiconductor/liquid interface. When interfacial electron-transfer rates become rate-limiting recombination processes, electron-transfer theories for the semiconductor/liquid interface predict a dependence of V_{oc} on the concentration of redox species.[20,43] Such concentration effects also have been predicted based on the numerical simulation of n-GaAs/Se^{2-}–KOH interfaces by Orazem and Newman.[44] We have measured V_{oc} for the n-Si/Me_2Fc–Me_2Fc^+–CH_3OH interface for several different concentration ratios of Me_2Fc/Me_2Fc^+ (Table II) and find negligible dependence of V_{oc} on $[Me_2Fc]/[Me_2Fc^+]$. The data in Table II indicate that measurements of V_{oc} at low concentrations of solution acceptor ions do not result in an artificial suppression of the recombination current (and consequent overestimation of V_{oc}) in the n-Si/CH_3OH–$Me_2Fc^{+/0}$ system. These data also conform to the expectations when the interfacial electron-transfer kinetics are rapid compared to the rate-limiting recombination current density for the system under AM1 conditions.

F. Chemical Reactivity Studies of the n-Si/CH_3OH Interface. We observe changes in V_{oc} for a number of redox systems after photoelectrochemical treatment of the n-Si. Figure 4 indicates measurements of V_{oc} vs. $E(A^+/A)$ for a series of outer-sphere redox couples in CH_3OH solvent. As reported previously,[14] we observe a region of linear dependence of V_{oc} vs. $E(A^+/A)$ for n-Si which has been HF etched, indicating that the n-Si Fermi level is substantially unpinned in CH_3OH solvent. After potential scanning to obtain steady-state current-voltage behavior in the n-Si/Me_2Fc–Me_2Fc^+–CH_3OH system,[1] a redetermination of V_{oc} vs. $E(A^+/A)$ for the same series of redox couples yields a profile shifted in potential by (–250) ± 50 mV, which again displays a region of linearly increasing V_{oc} up to the bulk diffusion/recom-

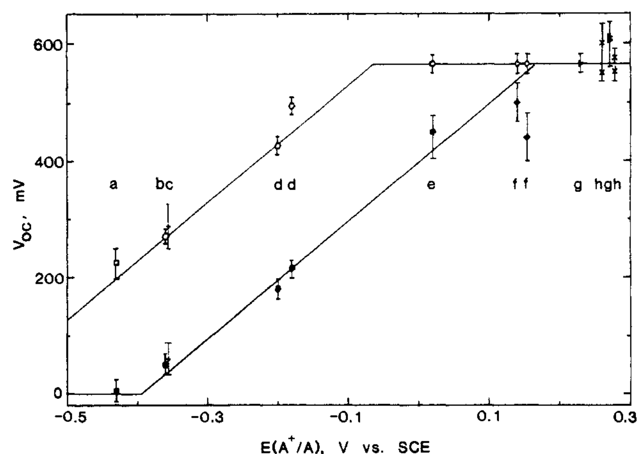

Figure 4. Comparison of the behavior before and after photoelectrochemical treatment of 1.5 Ω-cm n-Si photoelectrodes at ~ 100 mW/cm² in CH_3OH solution, using a measurement of the open-circuit photovoltage vs. solution redox potential. The lower (filled-in) symbol of each pair is the initial reading of V_{oc}, and the upper value is V_{oc} after the electrode has stabilized. The various redox couples used were as follows: (a) *N,N'*-dimethyl-4,4'-bipyridinium dichloride(2+/+) (in 1.0 M LiCl–CH_3OH), (b) *N,N'*-dibenzyl-4,4'-bipyridinium dibromide(2+/+) (in 1.0 M LiCl–CH_3OH), (c) 1,1'-(dicarbomethoxy)cobaltocene(+/0), (d) decamethylferrocene(+/0), (e) *N,N,N',N'*-tetramethylphenylenediamine-(+/0), (f) dimethylferrocene(+/0), (g) hydroxyethylferrocene(+/0), (h) ferrocene(+/0). The error bars reflect variations in temperature, solution absorption, intensity, and, in some cases, redox potential, while the duplicate designations for some redox systems reflect different ratios of reduced to oxidized forms of the redox couple.

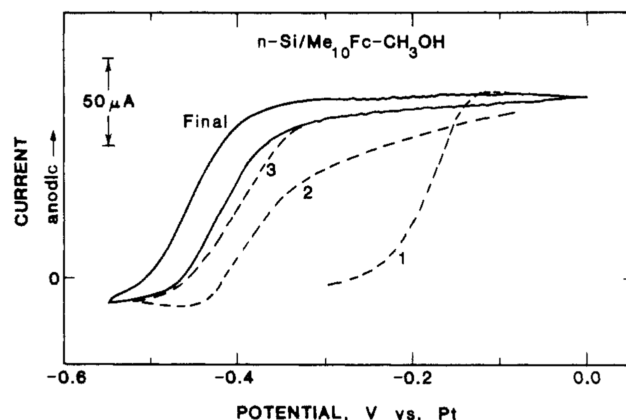

Figure 5. Current–voltage scans of 1.5 Ω-cm n-Si in 1.0 M $LiClO_4$–5.0 mM $Me_{10}Fc$–0.5 mM $Me_{10}Fc^+$–CH_3OH at scan rates of 50 mV/s: (---) initial three scans; (—) final scan after stabilization. The short-circuit current is mass transport limited and does not reflect the photocurrent under the 100 mW/cm² of ELH illumination. The open-circuit photovoltage increases from 205 to 510 mV.

(41) (a) Arora, J. D.; Mathur, C. *J. Appl. Phys.* **1981**, *52*, 3646. (b) Mathur, P. C.; Sharma, R. P.; Saxena, P.; Arora, D. *J. Appl. Phys.* **1981**, *52*, 3651.

(42) Hovel, H. J. In *Semiconductors and Semimetals*; Willardson, R. K., Beer, A. C., Eds.; Academic: New York, 1975; Vol. 11.

(43) (a) Gerischer, H. In *Physical Chemistry*; Eyring, M., Henderson, D., Yost, W., Eds.; Academic: New York, 1970; Vol. 9A. (b) Morrison, S. R. *Electrochemistry at Semiconductor and Oxidized Metal Electrodes*; Plenum: New York, 1981.

(44) Orazem, M. E.; Newman, J. *J. Electrochem. Soc.* **1984**, *131*, 2582.

bination limited value. An example of the shift in V_{oc} is provided in Figure 5, which depicts successive current–voltage scans in $Me_{10}Fc$–$Me_{10}Fc^+$–CH_3OH–$LiClO_4$ electrolyte. We attribute this behavior to a favorable shift in the flat-band potential due to adsorbed negative charge at the Si surface. We note that Howe[8b] has ascribed shifts in the flat-band potential at Si junctions to negative charge trapping in the oxide overlayer, and similar chemistry may be responsible for the effect observed here. Additionally, this interface must clearly possess a sufficiently low ratio of the rate of carrier recombination to the carrier injection rate into the solution to prevent interface state recombination from dominating the photocurrent–voltage characteristics under AM2 irradiation conditions. This favorable ratio of injected current to recombination current allows the bulk diffusion-limited voltage to be attained for redox systems with sufficiently positive electrochemical potentials.

We have also explored the effects of several chemical treatments which might affect the current–voltage properties of the n-Si/CH_3OH interface. Cardon and Gomes[45] have indicated that pH effects are pronounced for n-Si/CH_3OH interfaces and have observed shifts in photovoltage and in flat-band potential upon variation in pH. We observe that addition of acetic acid does not affect the photovoltage of the n-Si/$Me_2Fc^{+/0}$–CH_3OH system. We have also tested for incorporation of p-type dopants into the Si from the electrolyte ions. We observe essentially identical photovoltages for the n-Si/$Me_2Fc^{+/0}$–CH_3OH system using either $LiBF_4$, $[Et_4N^+][ClO_4^-]$, $[Et_4N^+][BF_4^-]$, or $LiClO_4$ electrolytes. This rules out spurious photovoltages due to the formation of an n–p junction from Li^+ ions in the electrolyte. The photovoltage is not affected by exposure to atmospheres containing dihydrogen, which might possibly act to passivate recombination sites or to induce interface dipoles and shift the flat-band potential. We have also investigated the properties of (111)-oriented, 1.5 Ω-cm resistivity n-Si substrates. Photoelectrochemical treatment of these samples is observed to produce bulk recombination/diffusion-limited voltages, but this process requires a somewhat longer immersion time for optimization than is typically required for (100)-oriented samples. The (111)-oriented Si surface is thought to have a somewhat larger density of states than the (100) surface with conventional oxidation; however, we observe that the surfaces yield similar V_{oc} values in contact with CH_3OH–$Me_2Fc^{+/0}$.

G. Surface Recombination Velocity Measurements. Our method of measurement of the surface recombination velocity of Si surfaces under low-level injection conditions was developed by Harten[46] and provides an opportunity to investigate the surface properties of the n-Si sample while in contact with CH_3OH. The method involves monitoring the photovoltage of a rectifying junction at the back of the n-Si wafer in response to variation in the wavelength of light incident on the front surface of the crystal (at the n-Si/liquid interface). The competition between carriers which recombine at the front surface and those which eventually produce a photovoltage at the back junction yields quantitative information on the front surface recombination velocity, S_f, and L_p. Harten has derived eq 3 to extract S_f from plots of the rear barrier photovoltage as a function of the photon penetration depth.

$$\eta_{int} = \frac{1}{\left(1 - \left(\frac{1}{\alpha(\lambda)L_p}\right)^2\right)}\left[\frac{A\exp(-d\alpha(\lambda)) - 1}{BL_p\alpha(\lambda)} - \frac{D_p}{S_fL_pB} + \exp(-d\alpha(\lambda))\right] \quad (3)$$

$$A = \cosh(d/L_p) + (D_p/S_fL_p)\sinh(d/L_p)$$

$$B = \sinh(d/L_p) + D_p/S_fL_p\cosh(d/L_p)$$

When a potential is applied between a Pt counter electrode and the back ohmic contact of the sample, S_f can be obtained as a function of the Si surface potential. A restriction on such measurements is that faradaic leakage pathways across the junction must be minimized in order to obtain meaningful S_f values.

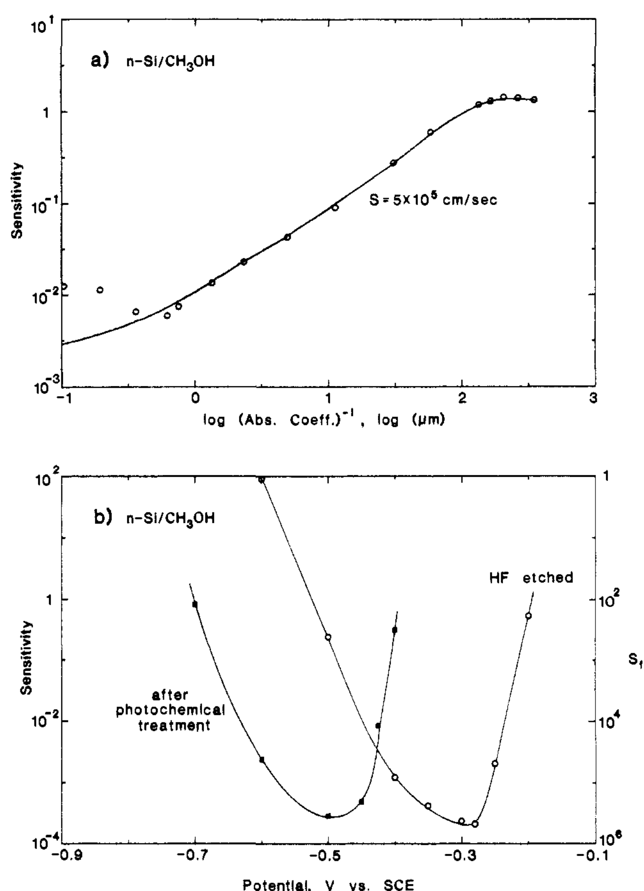

Figure 6. Determination of the low-level surface recombination velocity of photoelectrochemically treated 17 Ω-cm n-Si in 1.0 M LiCl–CH_3OH using the method of Harten.[46] (a) (O) Sensitivity (i.e., $(1/\eta_{int})$ vs. log (absorption coefficient)$^{-1}$. The electrode potential was maintained potentiostatically at −0.5 V vs. SCE, and the light intensity (typically ~1 μW/cm^2) was adjusted to maintain a constant photovoltage on the rear barrier junction. (b) Sensitivity at 450 nm (which is proportional to (surface recombination velocity)$^{-1}$) as a function of applied voltage (vs. Pt, measured relative to an SCE). (O) HF etched; (■) photoelectrochemically treated n-Si. The sensitivity in the anodic direction of the minimum was unstable and rising.

n-Si (HF-etched)/air junctions, and CH_3OH interfaces with (1) HF-etched n-Si and (2) HF-etched, photoelectrochemically treated, n-Si have been studied. A check of the procedure is that our measurements of S_f for the n-Si/air sample agree with the published value of $S = 10^4$ cm/s.[47] When the data at each applied voltage are fitted to eq 3, the maximum surface recombination velocity of the HF-etched n-Si/CH_3OH interface has been determined as 5×10^5 cm/s (Figure 6a). This is very close to the maximum value determined for an HF-etched Si sample in contact with an aqueous electrolyte.[48] Notably, this value is essentially unchanged after photoelectrochemical treatment in the n-Si/CH_3OH–Me_2Fc–Me_2Fc^+ system; thus, the improved V_{oc} behavior does not correlate with a decrease in the maximum low-level surface recombination velocity.

Analysis of the surface recombination velocity data for the n-Si/CH_3OH interface is interesting with respect to recent attempts to correlate changes in I–V behavior to variation in the surface recombination velocity.[21,22] Reference to the Shockley–Read–Hall equations for trap recombination[3,49,50] (eq 4) em-

(45) Brondeel, Ph.; Madou, M.; Gomes, W. P.; Cardon, F. *Sol. Energy Mater.* **1982**, *7*, 23.
(46) (a) Harten, H. U. *Philips Res. Rep.* **1959**, *14*, 346. (b) Harten, H. U. *J. Phys. Chem. Solids* **1960**, *14*, 220.
(47) Sah, C. T.; Lindholm, F. A. *Proc.—IEEE Photovolt. Spec. Conf.* **1976**, *12*, 93.
(48) Buck, T. M.; McKim, F. S. *J. Electrochem. Soc.* **1958**, *105*, 710.
(49) Many, A.; Goldstein, Y.; Grover, N. B. *Semiconductor Surfaces*; Wiley: New York, 1965.

phasizes several difficulties in the interpretation of S_f vs. V data.

$$R = v_{th} \int_{E_v}^{E_c} (p_s n_s - n_i^2) D_{it}(E_t) \times \left\{ \frac{1}{\sigma_p} \left[n_s + n_i \exp\left(\frac{E_t - E_i}{kT} \right) \right] + \frac{1}{\sigma_n} \left[p_s + n_i \exp\left(-\frac{E_t - E_i}{kT} \right) \right] \right\}^{-1} \mathrm{d}E_t \quad (4)$$

The subscript s refers to concentrations at the surface, D_{it} is the distribution of recombination centers as a function of energy, E_t is the energy in the band gap, σ is the capture cross section, E_i is the intrinsic Fermi energy, and v_{th} is the thermal velocity. The other symbols have their usual meanings. This expression reflects the steady-state trapping condition that recombination can only occur when both an electron and a hole have been captured by a trap site; thus, the denominator in eq 4 becomes large (and the steady-state trapping rate decreases) when traps are either fully occupied or fully empty.[49,50] It is clear that the recombination rate should depend dramatically on the surface potential due to changes in p_s and n_s. Thus, the general shape of the S_f vs. applied voltage curves in Figure 6b is evidence that the Fermi level is unpinned in CH_3OH solvent. Additionally, plots of S_f vs. V display a shift in the maximum S_f position of −200 mV after photoelectrochemical treatment of the Si surface. This is consistent with a constant dominant trap position and a negative shift in the flat-band position, in accord with the shift in V_{oc} vs. $E(A^+/A)$ plots observed in section F.

However, it is extremely difficult to relate low-level injection measurements of S_f at nonconducting interfaces to the S_f which is relevant at open circuit (under AM1 conditions) in contact with a redox system. Use of $S_f = 10^5$ cm/s in calculations of the surface recombination current ($J_{ss} = qp_sS_f$) yields an open-circuit voltage which is much lower than is actually observed at the n-Si/$Me_2Fe^{+/0}$–CH_3OH interface. Difficulties include the proper choice of the surface potential in the operating cell, changes in p_s and n_s with illumination intensity, the necessity to maintain charge neutrality for depleted interfaces in contact with nonconducting ambients,[50] and possible variations in σ_n/σ_p of greater than 10^7 with variation in the trap position.[51] Attempts to correlate S_f with I–V behavior will require detailed trap density and cross-section measurements for the interface under operating photoelectrochemical cell conditions.

An important point with regard to the liquid junction behavior is that an inversion layer (large p_s) will produce a small S_f even if D_{it} is large.[52] Thus, there is no contradiction between the high S_f values for certain surface potentials at the n-Si/CH_3OH interface and the excellent I–V behavior observed in the n-Si/$Me_2Fc^{+/0}$–$LiClO_4$–CH_3OH photoelectrochemical cell. For the redox systems used in this study, the low solvent reorganization energies should ensure rapid interfacial charge-transfer rates, allowing interfacial charge transfer to compete favorably with surface-related recombination processes.

(50) Henry, C. H.; Logan, R. A.; Merritt, F. R. *J. Appl. Phys.* **1978**, *49*, 3530.

(51) Eades, W. D. Ph.D. Thesis, June 1985, Stanford University, Stanford, CA.

(52) Green, M. A. *Appl. Phys. Lett.* **1978**, *33*, 178.

Conclusions

Kinetic studies of the n-Si/CH_3OH junction can successfully relate a microscopic description of the charge-transfer process to variation in the open-circuit photovoltage. V_{oc} for the n-Si/$Me_2Fe^{+/0}$–$LiClO_4$–CH_3OH junction is observed to be kinetically first order in photocurrent density, minority carrier diffusion length, and dopant density. The activation barrier for carrier transport is the band-gap energy of Si. These data indicate that the rate-determining kinetic process for this system is bulk diffusion/recombination. Rational manipulation of bulk semiconductor properties has led to semiconductor/liquid interfaces which display the highest photovoltage values for any n-Si-based solar device reported to date. Extremely high doping levels produce lower V_{oc} values due to excessive leakage currents through the thin surface barrier. Photoelectrochemical treatment of n-Si has been observed to introduce a surface dipole layer and to produce improvements in V_{oc}, but this treatment does not result in a decreased maximum surface recombination velocity at the n-Si/CH_3OH interface. Even with high trap densities, the presence of an inversion layer at a semiconductor/redox couple–liquid junction can yield low net surface recombination rates. In general, the effectiveness of surface recombination is related to the ratio of charge transfer across the interface to surface-oriented carrier recombination, and increases in this ratio will provide more efficient semiconductor/liquid junction interfaces.

Acknowledgment. We acknowledge the National Science Foundation, grant CHE-8312692, and the NSF Presidential Young Investigator Program for support of this work. N.S.L. also acknowledges support from PYI matching funds generously provided by Monsanto Co., the Exxon Educational Foundation, Mobil Corp., and the IBM Young Faculty Development Award Program and funds as an Alfred P. Sloan Foundation Fellow (1985–1987) and a Camille and Henry Dreyfus Teacher–Scholar (1985–1990). We also wish to thank Prof. Richard Swanson and Dr. Wendell Eades of Stanford University, Dr. Adam Heller of AT&T Bell Laboratories, and Dr. Karl Frese of SRI International for helpful discussions regarding surface recombination processes.

Registry No. Si, 7440-21-3; methanol, 67-56-1.